



Optics Letters

Direct readout of mirror reflectivity for cavity-enhanced gas sensing using Pound-Drever-Hall signals

HUI ZHANG,^{1,2}  DONGQING ZHANG,^{1,2} MENGPENG HU,^{1,2}  AND QIANG WANG^{1,2,*} 

¹State Key Laboratory of Applied Optics, Changchun Institute of Optics, Fine Mechanics and Physics, Chinese Academy of Sciences, Changchun 130033, China

²University of Chinese Academy of Sciences, Beijing 100049, China

*wangqiang@ciomp.ac.cn

Received 4 August 2023; revised 4 October 2023; accepted 22 October 2023; posted 23 October 2023; published 10 November 2023

The operation of cavity-enhanced techniques usually requires independent pre-calibration of the mirror reflectivity to precisely quantify the absorption. Here we show how to directly calibrate the effective mirror reflectivity without using any gas samples of known concentration or high-speed optical/electrical devices. Leveraging a phase modulator to generate sidebands, we are able to record Pound-Drever-Hall error signals shaped by cavity modes that can reveal the effective reflectivity after waveform analysis. As an example, we demonstrated the reflectivity calibration of a pair of near-infrared mirrors over 80 nm with a free spectral range-limited resolution, illustrating a reflectivity uncertainty of 2×10^{-5} in the center part of the reflection wavelength range of the mirrors and larger at the edges. With an effective reflectivity of 0.9982 (finesse ~ 1746) inferred at 1531.6 nm, a short ~ 8 -cm Fabry-Pérot cavity achieved a minimum detectable absorption coefficient of $9.1 \times 10^{-9} \text{ cm}^{-1}$ for trace C_2H_2 detection. This method, by providing convenient calibration in an almost real-time manner, would enable more practical cavity-enhanced gas measurement even with potential mirror reflectivity degradation. © 2023 Optica Publishing Group

<https://doi.org/10.1364/OL.501675>

Cavity-enhanced spectroscopic technology, due to its high sensitivity to intracavity absorption, has always held special appeal in a wide range of applications, such as biomedical research [1], atmospheric science [2,3], and breath diagnostics [4], for the precision analysis of target gas species. The high sensitivity relies on the significant interaction length extension between the laser and gas samples or the high laser power buildup by an optical cavity. The past years have witnessed rapid developments in the state-of-the-art cavity-enhanced techniques, such as cavity ringdown spectroscopy (CRDS) [1], cavity-enhanced absorption spectroscopy (CEAS) [2], noise-immune cavity-enhanced optical heterodyne molecular spectroscopy (NICE-OHMS) [5], doubly resonant photoacoustic spectroscopy [6], and cavity buildup dispersion spectroscopy (CBDS) [7]. The equivalent absorption path length can be extended from a given spatial scale of a dozen centimeters to a few kilometers. Similarly, the

laser power can be built up from a few milliwatts to hundreds of watts.

The reflectivity of cavity mirrors has an essential effect on both the equivalent absorption path length extension and the power buildup and subsequently the detection sensitivity. For high-reflectivity cavity mirrors ($>99\%$), a large fluctuation in the detection sensitivity would be introduced by even a small reflectivity change. Extra careful treatment, such as fine dust filters for gas sampling or mirror surface flushing using zero-absorption gas, has to be employed to prevent potential reflectivity degeneration, especially in field deployment [8]. Therefore, precision cavity-mirror reflectivity calibration is usually a previous work for most cavity-enhanced measurements [9].

Approaches to determine the wavelength-dependent mirror reflectivity $R(\lambda)$ can be mainly summarized as specific gas sample-assisted technologies and cavity ringdown (CRD) technologies. For former ones, recording the spectra of cavity transmission reveals $R(\lambda)$ by the synergy of the CEAS regime and concentration-known gas samples with certain absorption lines or by the synergy of Rayleigh scattering and different gas species with distinguishable scattering coefficients. The typical uncertainty in reflectivity calibration is limited to 10^{-2} – 10^{-4} [10,11], mainly owing to systematic errors from the uncertainty of sample concentration calibration or drifts in laser intensity. Except for the complicated operation, this approach is also restricted by the lack of calibrated samples in some spectral regions of interest and does not apply to scenarios, where sample gas cannot be stably contained, e.g., open-path configurations [12]. For CRD ones, the way of measuring the decay time of light leaking out of the cavity has a high laser intensity jitter immunity, serving as an ultrasensitive tool for reflectivity analysis. For instance, Rempe *et al.*, as early as 1992, reported a mirror reflectivity calibration of an ultrahigh finesse cavity up to 0.9999984 by CRD [13]. Furthermore, the no need of calibrated gas species benefits the fine-resolution reflectivity determination over a broad bandwidth with a low uncertainty down to 10^{-6} [14]. Meanwhile, the operation of CRD critically relies on high-speed optical/electrical devices, including optical switch, photodetector, and data acquisition board, due to the limited photon lifetime τ , i.e., ringdown time. Empirically, the effective system sampling rate at a sufficient bandwidth is often set to

be much higher than $1/\tau$ to minimize the fitting error in reflectivity inference. Hence, precision reflectivity calibration is very challenging and costly for the cavity-enhanced configuration if its ringdown time τ is estimated to be only a few μs , sub- μs , or much shorter [15], requiring a sampling rate up to GS/s level and laser beam switch down to the ns level. A long mirror distance would permit a longer ringdown time, however at the cost of coupling efficiency due to a much narrower cavity mode and gas consumption due to a larger cavity size [16]. Besides, the cavity-mirror reflectivity has a high possibility of degradation over time, especially when it is exposed to the target gas with dust grains or sticky components [16]. Complicated and frequent reflectivity recalibrations are necessary, which, however, are often the main causes for restricted performance of cavity-enhanced techniques, limiting their wider applications outside the laboratory.

In this Letter, we demonstrate an alternative approach to calibrate the effective mirror reflectivity without using any standard reference gas with known concentration or high-speed optical/electrical devices. An electro-optic phase modulator (EOM) is added before the optical cavity to generate sidebands so that scanning the laser source enables the recording of Pound–Drever–Hall (PDH) signal waveforms for further numerical mirror reflectivity analysis. By demonstrating the convenient reflectivity calibration for near-infrared mirrors as a proof-of-principle, this approach proves its capacity of direct mirror reflectivity calibration over a broad spectral band with a fine resolution, showing intriguing prospects in simplifying cavity-enhanced systems and improving reliability.

The PDH technique is a commonly used powerful tool that stabilizes the laser frequency to a stable optical cavity [17]. A PDH error signal, for the locking, is produced by two frequency modulation sidebands heterodyning with a carrier beam leaking out of the cavity resonance. Meanwhile, the cavity-finesse-dependent cavity mode shape can thus be mapped into the PDH signal waveform by scanning the carrier beam, bringing the new possibility of calibrating the effective mirror reflectivity in a more convenient way. For a Fabry–Pérot resonator as an example, its reflection coefficient $F(w)$ can be written as the ratio of E_i (the incident electric field) and E_r (the reflected electric field), which quantifies the behavior of the reflected beam. For an empty cavity, the expression, as derived by [18], is given by

$$F(w) = \frac{E_i}{E_r} = \frac{r \cdot \left(e^{\frac{2L-iw}{c}} - 1 \right)}{1 - r^2 \cdot e^{\frac{2L-iw}{c}}}, \quad (1)$$

where w is the angular laser frequency, L is the physical cavity length, c is the light velocity, and r is the amplitude reflection coefficient of each mirror, which is equal to $\sqrt{R(\lambda)}$.

When an EOM modulates the carrier laser at a frequency of $\Omega/2\pi$, the phase information in the reflected light can be demodulated by a mixer to extract the PDH signal as

$$\varepsilon = 2\sqrt{P_c \cdot P_s} \cdot \text{Im}[F(w)F^*(w + \Omega) - F^*(w)F(w - \Omega)], \quad (2)$$

where P_c is the power of the carrier beam and P_s for the sideband components, both of which are employed to yield the normalized waveform as $\varepsilon/2\sqrt{P_c \cdot P_s}$.

Figure 1(a) shows the simulation results of PDH error signals for different cavity-mirror reflectivity from 0.995 to 0.999 with a cavity length of 8 cm and a phase modulation frequency of 20 MHz. The different signal waveforms confirm the possibility

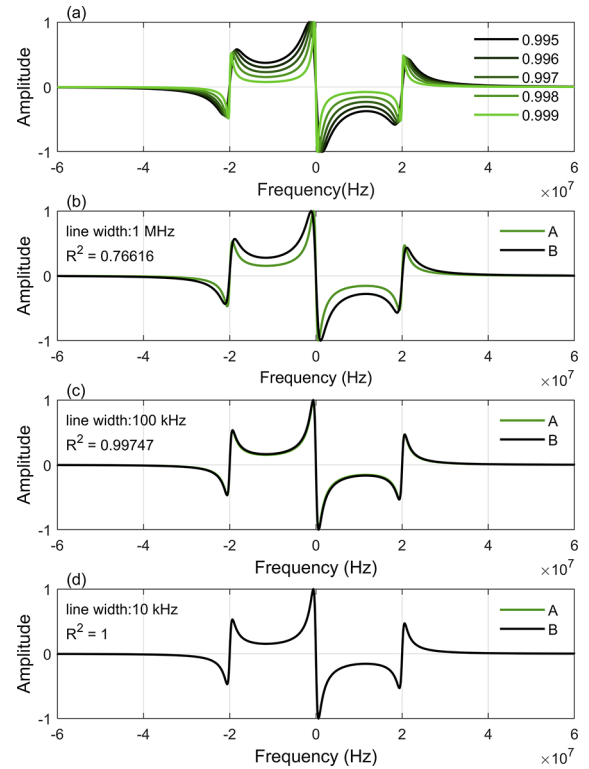


Fig. 1. (a) Simulation results of PDH error signals for different reflectivities of cavity mirrors. (b)–(d) Simulation results of PDH error signals at a certain reflectivity of 0.998 (cavity mode linewidth ~ 1.19 MHz) with and without considering the effects of laser linewidth, 1 MHz, 100 kHz, and 10 kHz, respectively. Condition A (labeled by $\color{green}\rightarrow$): without considering the laser linewidth; condition B (labeled by $\color{black}\rightarrow$): with considering the laser linewidth.

of calibrating the effective mirror reflectivity by fitting the PDH signal.

It is worth mentioning that the laser linewidth effect could also be superimposed on PDH signal waveforms due to the laser-optical cavity convolution in heterodyne detection. To improve the measurement accuracy, it is necessary to assess its influence on PDH signal waveforms. For the incident laser with a center frequency of w_0 , the reflection function expression by the resonator becomes [19]

$$F'(w) = F(w) * H(w), \quad (3)$$

where $H(w)$ is the line shape function of the incident laser. The convolution of a transmission function with a line shape function results in one function smoothing and broadening the other, and Eq. (2) becomes

$$\frac{\varepsilon}{2\sqrt{P_c \cdot P_s}} = \text{Im}[F'(w)F'^*(w + \Omega) - F'^*(w)F'(w - \Omega)]. \quad (4)$$

Figures 1(b)–1(d) depict the simulation results with and without considering the laser linewidth for a cavity length of 80 mm and a certain reflectivity of 0.998, which corresponds to a mode linewidth (full width at half maximum, FWHM) of 1.19 MHz. Note that a Lorentzian profile is selected as the line shape function of the incident laser for convenience [20]. The PDH signals, shown in Fig. 1(b), obviously separate each other when the laser linewidth approaches to the same order of magnitude as the cavity mode FWHM. It has a similar behavior to the results

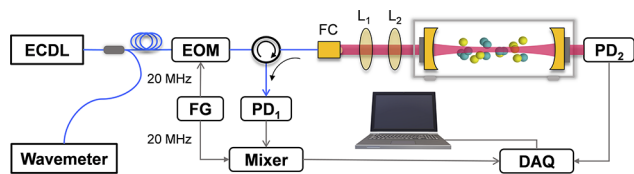


Fig. 2. Schematic view of experimental setup for the direct cavity-mirror reflectivity calibration. ECDL, external cavity diode laser; EOM, electro-optic phase modulator; FG, function generator; FC, fiber collimator; $L_{1,2}$, mode-matching lens; $PD_{1,2}$, photodetector; DAQ, data acquisition card.

in Fig. 1(a) in the direction of decreasing reflectivity. When the laser linewidth is 100 kHz, the two curves in Fig. 1(c) hold a high consistency with the coefficient of determination calculated to be $R^2 = 0.9975$. Needless to say, it hardly makes a difference with a linewidth of 10 kHz shown in Fig. 1(d). Therefore, the simulation results confirm that the laser linewidth effect could be ignored if it is less than a tenth of the cavity mode linewidth. Otherwise, precision reflectivity calibration needs the laser linewidth to be taken into account.

The experimental setup for the proposed cavity-mirror reflectivity calibration is shown in Fig. 2. The short Fabry-Pérot resonant cavity consists of two mirrors (Layertec, reflectivity: $0.998 + 0.0015/-0.003$ at 1560 nm) with a radius of curvature of 150 mm, a cavity length of ~ 80 mm, and a moderate reflectivity, yielding a free spectral range (FSR) of ~ 1.875 GHz and a cavity mode linewidth of about MHz level. Note that the ring-down time τ could be expected to be about tens to hundreds of nanoseconds, which is pretty challenging to accurately calibrate its reflectivity even for the mature CRD techniques. An external cavity diode laser (ECDL) with a narrow linewidth of 5–10 kHz is used as the laser source, which has a wide mode-hop-free spectral tunability. An EOM modulates the laser at 20 MHz to generate the optical sidebands. By using a fiber collimator and a pair of mode-matching lenses, the laser is coupled to the optical resonator. The reflected laser beam from the optical cavity is picked out by a circulator and then collected by a photodetector (PD_1). The PD signal is mixed with a 20 MHz reference from the same function generator that drives the EOM. Another photodetector (PD_2) captures the cavity transmission.

A LabVIEW program is developed for mirror reflectivity calibration by the successive PDH error signal acquisition,

normalization, and mathematic derivation process. We locate the center frequency ($\nu_0 = 0$ Hz) and the sidebands (± 20 MHz) by interrogating the position of the extreme points and thus scale the frequency of the horizontal axis. Finally, the reflectivity can be conveniently obtained by fitting the processed signals with the Levenberg–Marquardt algorithm. Figure 3 demonstrates a broadband effective reflectivity curve of the cavity mirrors acquired by scanning the wavelength of ECDL from 1510 nm to 1591 nm at a tuning speed of 0.5 nm/s. The representative results of 0.9982 with an uncertainty of 2×10^{-5} at 1531.6 nm and 0.9851 with an uncertainty of 3.1×10^{-4} at 1590 nm are shown in Figs. 3(a) and 3(c), respectively. The uncertainty was obtained by calculating the standard deviation (1σ) of 500 continuous measurements as shown in Fig. 3(b). It is of interest that the uncertainty increases as the mirror reflectivity decreases, which is similar to reflectivity calibration techniques using CRD [21] (see Supplement 1).

We further investigated the reliability of this proposed direct cavity-mirror reflectivity calibration by exploring the spectral response to concentration-calibrated trace gases in a CEAS manner. Quantitative analysis of the cavity-enhanced transmission spectra can only be performed with the knowledge of the cavity length and the mirror reflectivity. Its mirror reflectivity was determined from the results in Fig. 3. Its cavity length L , assumed to be equal to $c/(2 \cdot \text{FSR})$, was determined to be 79.6 mm by measuring the FSR with a wavemeter shown in Fig. 2, yielding an effective absorption path length of 88.4 m. Choosing C_2H_2 as an example for demonstration, we tuned the wavelength to 1531.6 nm to exploit the absorption line (P11) at 6529.172 cm^{-1} . Gas samples were prepared by diluting the certified 999 ppm C_2H_2/N_2 mixture with pure N_2 . Figure 4(a) shows the transmission spectra of C_2H_2 with different concentrations at atmospheric pressure and room temperature. With known mirror reflectivity and cavity length, we calculated the C_2H_2 concentrations by analyzing the absorption spectra. The results are shown in Fig. 4(b), which agree very well with the calibrated gas concentrations. The absolute residues are below 2.2 ppm, which may be caused by the synergy of the reflectivity calibration error, the gas dilution uncertainty, and the spectral fitting error.

To evaluate the detection sensitivity and long-time stability, an Allan–Werle deviation analysis was conducted by continuously monitoring pure N_2 at the line center for over 1 h with a sampling rate of 10 S/s, as shown in Fig. 4(c). The noise equivalent

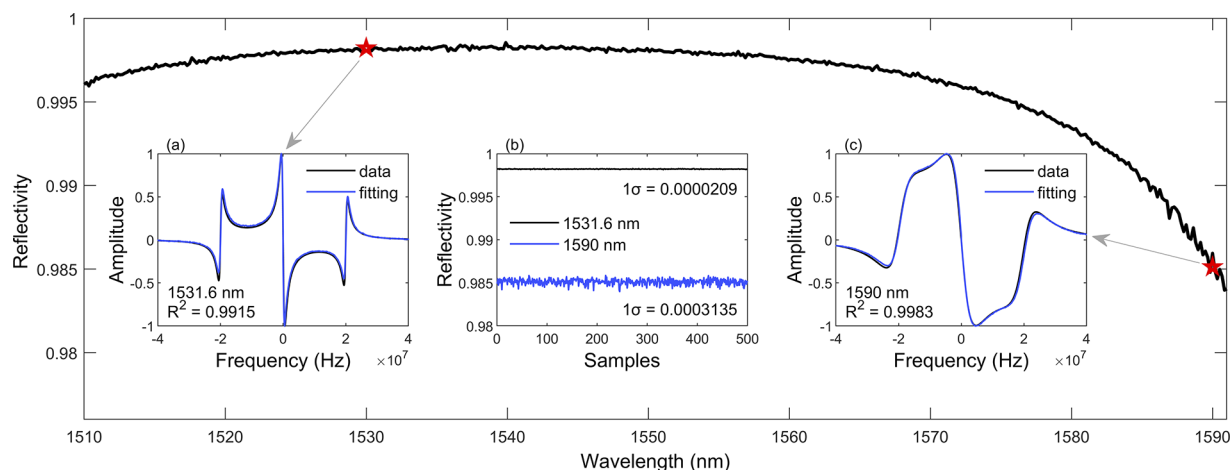


Fig. 3. Broadband (1510–1591 nm) effective reflectivity of the cavity mirrors. Inset: representative error signals: measurement and fitting by Levenberg–Marquardt algorithm at (a) 1531.6 nm and (c) 1590 nm; (b) continuous measurement of the reflectivity.

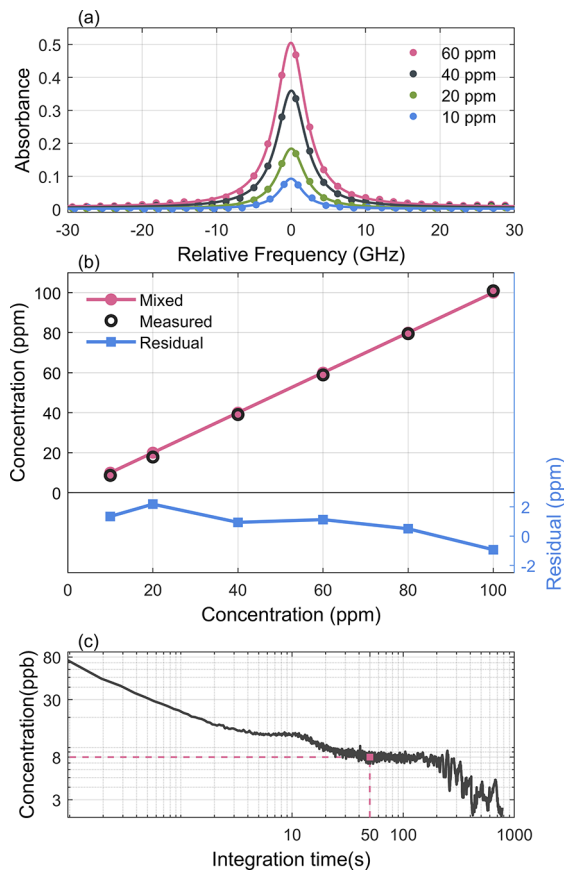


Fig. 4. (a) Representative cavity-enhanced absorption spectra of C_2H_2 measured at different concentrations; solid lines: fitted by the Lorentzian profile. (b) Concentration of mixed gas versus the measured concentration. The residuals are plotted at the bottom panel. (c) Allan–Werle deviation analysis.

concentration (NEC) is determined to be 8 ppb at an integration time of 50 s, leading to a minimum detectable absorption coefficient (MDA) of $9.1 \times 10^{-9} \text{ cm}^{-1}$.

In conclusion, this Letter demonstrates a convenient approach for cavity-mirror reflectivity calibration without using any gas samples of known concentration or high-speed optical/electrical devices. Harnessing a common EOM enables the capture of PDH error signal waveforms, into which the cavity mode features have been mapped, for further reflectivity inference. By scanning the laser wavelength, we have measured the effective reflectivity of a pair of cavity mirrors with a measurement range of 0.9849–0.9984 (see Supplement 1) over a wide range (80 nm), an FSR-limited resolution (1.8846 GHz), and an uncertainty of as low as 2×10^{-5} . The independent accurate concentration retrieval for calibrated gas samples further confirms its reliability. Our results hold promise for easy precision reflectivity calibration in an almost real-time manner, in particular when only moderate reflectivity and/or confined cavity geometry can be expected, despite a challenging ns-level ringdown time for conventional CRD techniques. This simple approach will benefit the development of practical cavity-enhanced techniques for

many scenarios, where, e.g., high-performance auxiliary instruments of interest are not always available or potential reflectivity variation exists in the field deployment.

Funding. Natural Science Foundation of Jilian Providence (SKL202302022); National Natural Science Foundation of China (62005267).

Disclosures. The authors declare no conflicts of interest.

Data availability. Data underlying the results presented in this paper are not publicly available at this time but may be obtained from the authors upon reasonable request.

Supplemental document. See Supplement 1 for supporting content.

REFERENCES

- I. Galli, S. Bartalini, R. Ballerini, M. Barucci, P. Cancio, M. De Pas, G. Giusfredi, D. Mazzotti, N. Akikusa, and P. De Natale, *Optica* **3**, 385 (2016).
- N. Jordan and H. D. Osthoff, *Atmos. Meas. Tech.* **13**, 273 (2020).
- H. Chen, J. Winderlich, C. Gerbig, A. Hofer, C. W. Rella, E. R. Crosson, A. D. Van Pelt, J. Steinbach, O. Kolle, V. Beck, B. C. Daube, E. W. Gottlieb, V. Y. Chow, G. W. Santoni, and S. C. Wofsy, *Atmos. Meas. Tech.* **3**, 375 (2010).
- L. Ciaffoni, G. Hancock, J. J. Harrison, J.-P. H. van Helden, C. E. Langley, R. Peverall, G. A. D. Ritchie, and S. Wood, *Anal. Chem.* **85**, 846 (2013).
- G. Zhao, T. Hausmaninger, W. Ma, and O. Axner, *Opt. Lett.* **43**, 715 (2018).
- Z. Wang, Q. Wang, H. Zhang, S. Borri, I. Galli, A. Sampaolo, P. Patimisco, V. L. Spagnolo, P. De Natale, and W. Ren, *Photoacoustics* **27**, 100387 (2022).
- A. Cygan, A. J. Fleisher, R. Ciurylo, K. A. Gillis, J. T. Hodges, and D. Lisak, *Commun. Phys.* **4**, 14 (2021).
- Y. He, C. Jin, R. Kan, J. Liu, W. Liu, J. Hill, I. M. Jamie, and B. J. Orr, *Opt. Express* **22**, 13170 (2014).
- M. Triki, P. Cermak, G. Méjean, and D. Romanini, *Appl. Phys. B* **91**, 195 (2008).
- J. Chen and D. S. Venables, *Atmos. Meas. Tech.* **4**, 425 (2011).
- D. S. Venables, T. Gherman, J. Orphal, J. C. Wenger, and A. A. Ruth, *Environ. Sci. Technol.* **40**, 6758 (2006).
- R. M. Varma, D. S. Venables, A. A. Ruth, U. Heitmann, E. Schlosser, and S. Dixneuf, *Appl. Opt.* **48**, B159 (2009).
- G. Rempe, R. J. Thompson, H. J. Kimble, and R. Lalezari, *Opt. Lett.* **17**, 363 (1992).
- T. Laurila, I. S. Burns, J. Hult, J. H. Miller, and C. F. Kaminski, *Appl. Phys. B* **102**, 271 (2011).
- D. K. Armani, T. J. Kippenberg, S. M. Spillane, and K. J. Vahala, *Nature* **421**, 925 (2003).
- G. Gagliardi and H.-P. Loock, eds., *Cavity-Enhanced Spectroscopy and Sensing*, Springer Series in Optical Sciences (Springer Berlin Heidelberg, 2014), p. 179.
- Z. Wang, Q. Wang, W. Zhang, H. Wei, Y. Li, and W. Ren, *Opt. Lett.* **44**, 1924 (2019).
- E. D. Black, *Am. J. Phys.* **69**, 79 (2001).
- V. L. Kasyutich and M. W. Sigrist, *Infrared Phys. Technol.* **71**, 179 (2015).
- L. L. Strow, *J. Quant. Spectrosc. Radiat. Transfer* **29**, 395 (1983).
- L. Gao, S. Xiong, B. Li, and Y. Zhang, in *Advances in Optical Thin Films II* (SPIE, 2005), pp. 660–667.